

# The Molecular Second Hyperpolarizability of the Light-Harvesting Chlorophyll *a/b* Pigment–Protein Complex of Photosystem II

Danielle Tokarz,<sup>†,‡</sup> Richard Cisek,<sup>†,§</sup> Ulrich Fekl,<sup>†,‡</sup> and Virginijus Barzda<sup>\*,†,‡,§</sup>

<sup>†</sup>Department of Chemical and Physical Sciences, University of Toronto Mississauga, 3359 Mississauga Road North, Mississauga, ON, Canada L5L 1C6

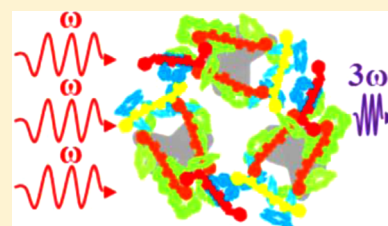
<sup>‡</sup>Department of Chemistry, University of Toronto, 80 St. George Street, Toronto, ON, Canada M5S 3H6

<sup>§</sup>Department of Physics and Institute for Optical Sciences, University of Toronto, 60 St. George Street, Toronto, ON, Canada M5S 1A7

## S Supporting Information

**ABSTRACT:** Photosynthetic structures when imaged with nonlinear optical microscopy give rise to high third harmonic generation (THG) signal intensity due to the presence of chlorophylls and xanthophylls which have large second hyperpolarizability ( $\gamma$ ) values. The  $\gamma$  value of trimers of the light-harvesting chlorophyll *a/b* pigment–protein complex of photosystem II (LHCII) isolated from pea (*Pisum sativum*) plants was investigated by the THG ratio technique at 1028 nm wavelength and found to have the value  $(-1600 \pm 400) \times 10^{-41} \text{ m}^2 \text{ V}^{-2}$ . The large negative  $\gamma$  value of trimeric LHCII is due to the presence of chlorophyll *a* and chlorophyll *b* which have large negative  $\gamma$  values, while positive  $\gamma$  values of xanthophylls reduce the magnitude of the THG signal.

Variation was observed between the measured  $\gamma$  value of LHCII and the approximated  $\gamma$  value of LHCII obtained by adding individual  $\gamma$  values of chlorophylls and xanthophylls. This difference can be attributed to the differing inter-pigment interactions of oriented chlorophylls and xanthophylls in the pigment–protein complex compared to randomly oriented non-interacting pigments in solution, as well as a differing dielectric environment of the pigments within LHCII versus the surrounding organic solvent.



## ■ INTRODUCTION

Third harmonic generation (THG) microscopy is a valuable technique used to image biological structures without staining. THG is produced at an interface where a difference in the refractive index or third-order nonlinear susceptibility ( $\chi^{(3)}$ ) is present. The third-order nonlinear susceptibility is related to the molecular second hyperpolarizability ( $\gamma$ ), and is dependent upon the concentration and arrangement of molecules in the biological structure. In particular, carotenoids<sup>1,2</sup> and porphyrin-like<sup>3</sup> molecules have been shown to have  $\gamma$  values with large magnitudes. Therefore, photosynthetic samples tend to give rise to strong THG signal, which can be used to study pigment–pigment and pigment–protein interactions in photosynthetic complexes with different compositions of pigments and altered protein structures.

Previous examples of photosynthetic samples imaged with THG microscopy include plant leaf cells<sup>4</sup> and rhizoids from green algae<sup>5</sup> both performed with a fundamental wavelength of 1200 nm. As well, THG imaging of chloroplasts have been performed at 1560 nm,<sup>6</sup> 1230 nm,<sup>7</sup> 1028 nm<sup>8</sup> and 800 nm<sup>9</sup> excitation. The strong THG signal from chloroplasts was attributed to the high concentration of chlorophyll present in chloroplasts.<sup>6</sup> THG has been shown to be efficiently generated at 840 nm<sup>10</sup> and 1028 nm<sup>8</sup> excitation in aggregates of the light-harvesting chlorophyll *a/b* pigment–protein complex of photosystem II (LHCII), the most abundant pigment–protein complex in chloroplasts.<sup>11</sup> LHCII is located at the periphery of

the light harvesting antenna of photosystem II and is involved in the regulation of the absorbed energy flow to the reaction centers.<sup>12–15</sup> THG signal from LHCII is believed to be generated due to the presence of chlorophylls and xanthophylls.<sup>8</sup> Second, hyperpolarizability studies of xanthophylls and chlorophylls with a fundamental wavelength at 1028 nm have revealed that chlorophylls have larger absolute  $\gamma$  values than xanthophylls as well as chlorophylls have negative  $\gamma$  values while xanthophylls have positive  $\gamma$  values.<sup>16,17</sup> Therefore, one would expect that a pigment–protein complex such as LHCII, which contains both xanthophyll and chlorophyll molecules, would lead to partial THG cancellation.<sup>17</sup>

In this paper, LHCII was taken as a model system of a pigment–protein complex, and the  $\gamma$  value of an LHCII trimer was measured for the first time by employing the THG ratio technique along with refractive index measurements. The THG intensity at a solution–glass interface and a glass–air interface of a glass capillary tube was determined and used to calculate the third-order nonlinear susceptibility ( $\chi^{(3)}$ ) of a suspension of LHCII trimers in buffer solution. The  $\gamma$  value of trimeric LHCII was then deduced by measuring the  $\chi^{(3)}$  at numerous

**Special Issue:** Rienk van Grondelle Festschrift

**Received:** January 22, 2013

**Revised:** April 12, 2013

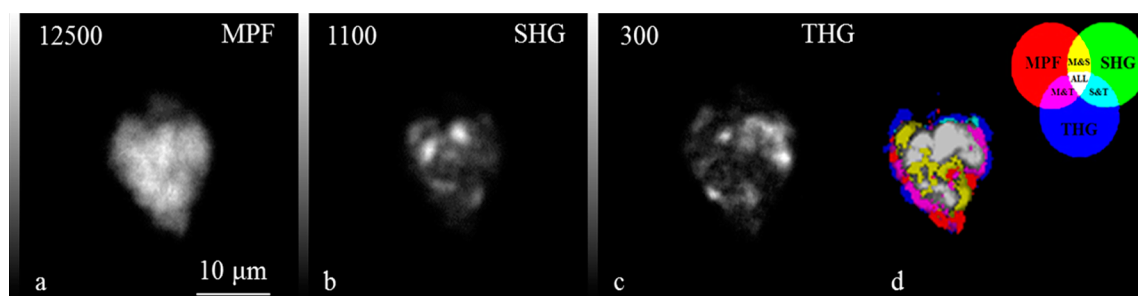


**Figure 1.** Nonlinear optical microscopy images of LHCII aggregates isolated from pea (*Pisum sativum*) leaves visualizing (a) MPF, (b) SHG, and (c) THG where the numbers in the upper left corner indicate the maximum photon counts in a pixel and the gray scale bar on the left side of the image ranges from 0 to the maximum signal intensity. A structural image cross-correlation analysis<sup>9</sup> between MPF, SHG, and THG was performed and is demonstrated in image (d).

concentrations. The measured  $\gamma$  value of LHCII appeared to be large and negative, providing evidence that the predominant origin of THG is due to the presence of chlorophyll molecules in the pigment–protein complexes. The obtained  $\gamma$  value of an LHCII trimer can serve as a reference when characterizing the THG intensity from other pigment–protein complexes. The comparison of the  $\gamma$  values from photosynthetic proteins, which contain different organizations of chlorophylls and carotenoids, can provide information about the pigment interactions within the pigment–protein complexes. Mutants of pigment–protein complexes and complexes reconstituted with different amounts of photosynthetic pigments can be employed to deduce inter-pigment interactions using second hyperpolarizability measurements. The photosynthetic pigments can also be used for creating labels known as harmonophores for third harmonic generation microscopy. Understanding the inter-pigment interactions in photosynthetic light-harvesting antenna may help in designing more efficient harmonophores.

## ■ EXPERIMENTAL METHODS

**LHCII Preparations.** LHCII was isolated from the leaves of two week old pea (*Pisum sativum*) plants as described by Simidjiev et al.<sup>18</sup> Briefly, isolated thylakoid membranes were solubilized with 0.8% of a 20% Triton X-100 solution buffered with 20 mM Tricine/NaOH at pH 7.8, and centrifuged at 30,000 g for 40 min to remove the insoluble pellet. LHCII was subsequently precipitated with 20 mM of  $\text{MgCl}_2$  and 100 mM KCl, and purified by centrifugation of the LHCII suspension layered above a 0.5 M sucrose layer. The sediment of LHCII aggregates was resuspended with a concentration of 0.9 mg/mL chlorophyll *a* + *b* by Arnon<sup>19</sup> and then solubilized with 1.0% of a 10% Triton X-100 solution buffered with 15 mM Tricine/KOH at pH 7.8, precipitated with 20 mM of  $\text{MgCl}_2$  and 100 mM KCl, and purified by centrifugation of the LHCII suspension layered above a 0.5 M sucrose layer. Final purification was performed via further aggregation with 20 mM of  $\text{MgCl}_2$  and 100 mM KCl, and purified by centrifugation of the LHCII suspension layered above a 100 mM sorbitol layer followed by repeated washing to obtain a chlorophyll *a/b* ratio between 1.1 and 1.2. The chlorophyll concentration was measured according to the method developed by Arnon.<sup>19</sup> The UV–vis spectral measurements were performed with an OLIS-14 upgraded Cary-14 spectrophotometer. Samples were stored at 4 °C in the dark and were used within one week after isolation.

In order to ensure that the suspension contained only trimers of LHCII, the LHCII aggregates with a concentration of 20  $\mu\text{g}/$

mL chlorophyll *a* + *b* were solubilized with the critical micelle concentration of Triton X-100 which corresponded to 0.025% v/v, and the aggregation state was verified with circular dichroism (CD) spectroscopy (Aviv 215 circular dichroism spectrometer).<sup>20</sup> At a higher concentration of LHCII (80  $\mu\text{g}/$  mL chlorophyll *a* + *b*) the critical micelle concentration shifted to 0.03% v/v of Triton X-100.

**Nonlinear Optical Microscope.** Imaging of LHCII was performed with the nonlinear optical multicontrast microscope, which has been described elsewhere.<sup>21</sup> Briefly, the laser source consisted of a home-built  $\text{Yb:KGd}(\text{WO}_4)_2$  oscillator, which provided  $\sim 450$  fs duration pulses emitting at a wavelength of 1028 nm with a pulse repetition rate of 14.3 MHz.<sup>22</sup> A high numerical aperture (NA) air objective (0.75 NA, Zeiss) was used. Multiphoton excitation fluorescence (MPF), second harmonic generation (SHG) and THG imaging was conducted simultaneously. MPF was obtained with epi-detection. Three short wavepass filters (SPF-750, CVI Melles Griot) and one color glass filter (RG-665, CVI Melles Griot) was placed in front of the photomultiplier tube for separation of fluorescence from the laser radiation in MPF studies of LHCII and chlorophyll solutions in acetone, while for MPF studies of xanthophyll solutions in acetone, the color glass filter was replaced with OG-530 (CVI Melles Griot). SHG and THG signal was collected in the forward direction through a home-built UV transmitting objective, split with a dichroic mirror, and filtered with a band-pass interference filter (F10–514.5, CVI Melles Griot) and a color glass filter (BG-39, CVI Melles Griot) for SHG and F10–340 (CVI Melles Griot) for THG. The signals were measured using photon-counting detectors (MPF and SHG: H7421–40, Hammamatsu and THG: MP–1343, Perkin Elmer).

**$\chi^{(3)}$  Measurements.** The nonlinear optical microscope was modified in order to find the  $\chi^{(3)}$  of a solution.<sup>16,17</sup> A 0.25 NA objective (Zeiss) was used for excitation during second hyperpolarizability measurements in order to minimize optical aberrations from higher NA objectives.<sup>23</sup> A capillary tube (W5010, VitroCom) was used to contain the solutions. For THG ratio measurements, the capillary tube was translated axially, and the THG signal generated from the two interfaces (solution-glass and glass-air) closest to the collection objective were recorded.<sup>17</sup> In order to determine the  $\chi^{(3)}$  of a solution, an equation expressing the  $\chi^{(3)}$  ratio by Shcheslavskiy et al. was applied.<sup>24</sup> Previously published values for the refractive indices and the  $\chi^{(3)}$  value of Duran borosilicate glass were used.<sup>16</sup> The  $\gamma$  value was then extracted from the plot of  $\chi^{(3)}$  versus concentration.<sup>25,26</sup>

Refractive indices of LHCII suspensions were measured using a home-built UV to near IR refractometer described elsewhere.<sup>17</sup> Briefly, a 450 W xenon arc lamp (LH-450, SLM Instruments) coupled to a monochromator (MC320/H, SLM Instruments) achieved wavelength tuning between 260 and 1030 nm. Light was transmitted through two YAG prisms (Red Optonics) and a spacer containing two solutions simultaneously: the sample solution and water. Light was detected by a standard CMOS camera while the prisms were rotated on a rotation stage (481-A, Newport) until the light diminished due to the total internal reflection at the YAG solution interface. The critical angles found for the LHCII suspension and water were used to calculate the refractive index of the LHCII suspension.

## RESULTS/DISCUSSION

**Nonlinear Microscopy of LHCII Aggregates.** Prior to measuring the  $\gamma$  value of LHCII trimers, LHCII aggregates isolated from pea (*Pisum sativum*) leaves were investigated with multicontrast MPF, SHG, and THG microscopy (Figure 1).

Signals from the three contrast mechanisms highlight different features of the LHCII aggregate.<sup>8</sup> The MPF signal from the LHCII aggregate results from two-photon excitation of chlorophylls and carotenoids in the pigment–protein complexes, as determined by the quadratic dependence of fluorescence signal on laser intensity (see Supporting Information Figure 1). The MPF image demonstrates a rather homogeneous distribution of LHCII (Figure 1a), where the MPF signal intensity varies 30% indicating very similar quenching properties as well as density of the pigment–protein complexes in the aggregate. The SHG signal from the LHCII aggregate (Figure 1b) visualizes domains with noncentrosymmetrically arranged xanthophylls and chlorophylls. LHCII aggregates are known to exhibit strong CD.<sup>9</sup> In this preparation, CD revealed that LHCII is likely to be found in two-dimensional (2D) lamellar aggregates<sup>20</sup> (CD spectrum not shown). The pigment–protein complexes can aggregate into unilamellar stacks arranged in a unidirectional fashion, which would generate strong SHG signal. Figure 1b shows that the SHG domains are embedded in a more centrosymmetrically arranged LHCII aggregate. Lastly, THG signal from the LHCII aggregate is attributed to the presence of xanthophylls and chlorophylls, which have high  $\gamma$  values. Unlike SHG, THG does not have organizational constraints and rather, THG signal requires structural heterogeneity occurring at interfaces where a change in refractive index and  $\chi^{(3)}$  takes place. Multilamellar structures, such as stacks of thylakoid membranes can enhance the THG signal.<sup>8,9,27</sup>

Correlation between MPF signal and SHG or THG signal of the LHCII aggregate demonstrates evidence showing that harmonic signals are generated from the pigment–protein complexes. SHG and THG signals are mostly anticorrelated. Stronger SHG signal is seen in regions of weaker THG signal, and weaker SHG signal is seen in regions of stronger THG. This observation has been previously described and explained by originating from the multilamellar structure of LHCII aggregates.<sup>9</sup> The most intense SHG is observed in unidirectionally arranged stacks of membranes oriented parallel to the optical axes. At this orientation, the LHCII aggregates also show the largest chirality of the structure.<sup>9</sup> Conversely, THG is most intense when the multilayer structure of LHCII is oriented perpendicular to the laser beam.<sup>9</sup>

**Aggregation Dependent THG Signals of LHCII.** The third-order nonlinear optical properties of LHCII were further investigated by studying the THG intensity ratio of solution-glass to glass-air interfaces using the multicontrast nonlinear optical microscope. The THG ratios for LHCII at different aggregation states were obtained by varying the Triton X-100 concentration in the LHCII suspension (Figure 2). For an

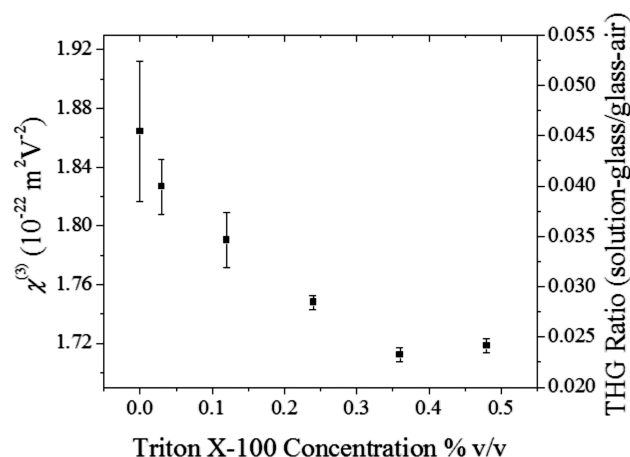


**Figure 2.** The third-order nonlinear susceptibility and the THG ratio intensity for an 80  $\mu\text{g/mL}$  chlorophyll *a + b* solution of aggregated LHCII at various Triton X-100 concentrations. At 0.03% v/v Triton X-100 concentration LHCII exists in trimeric form and at 0.12% v/v concentration in monomeric form, as determined by CD spectroscopy.<sup>29</sup>

LHCII sample containing no detergent, the THG intensity ratio data were ignored when aggregates larger than the excitation focal volume occurred in the focus of the microscope objective. Therefore, the THG intensity at 0% v/v Triton X-100 corresponds to smaller aggregates contained in the suspension.

In order to calculate the  $\chi^{(3)}$  of the LHCII suspension, the refractive indices were measured at two wavelengths: the fundamental wavelength of the laser, 1028 nm, and the third harmonic wavelength, 343 nm. Refractive index measurements of Triton X-100 in buffer at concentrations of interest did not significantly change from the refractive indices of the buffer, therefore the same refractive indices were assumed for the LHCII suspensions containing different detergent concentrations.

As the Triton X-100 concentration increases, the size of LHCII aggregates present in solution decreases, and, as a result, the THG intensity ratio and the  $\chi^{(3)}$  of the aggregated LHCII suspension decreases. This indicates that larger LHCII aggregates show stronger THG signal. This is in agreement with previous research, which suggested that the enhancement of THG signal can be achieved with the aggregation of hematocytin.<sup>28</sup>

At concentrations of Triton X-100 above the critical micelle concentration (0.03% v/v) LHCII disaggregates into trimers, while LHCII monomers start to appear gradually at higher Triton X-100 concentrations.<sup>29</sup> At concentrations above 0.36% v/v, the release of some pigments from LHCII is likely to occur. The THG ratio increase observed above 0.36% v/v of the detergent concentration is consistent with previously shown data of a larger THG ratio for chlorophylls in acetone.<sup>17</sup>



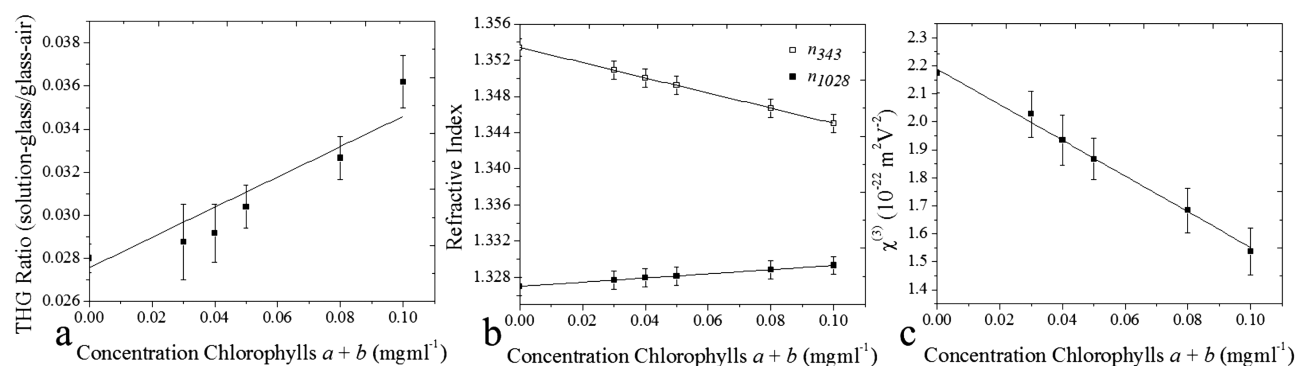


**Figure 3.** Determination of the second hyperpolarizability from the concentration dependent THG ratio and refractive index difference measurements of LHCII trimers in buffer solubilized with 0.025% v/v Triton X-100: (a) the THG intensity ratio for LHCII versus concentration of chlorophylls *a* + *b*, (b) refractive indices of LHCII in buffer solution taken at 343 and 1028 nm, and (c)  $\chi^{(3)}$  plot versus concentration of chlorophylls *a* + *b*.

**Determination of the  $\gamma$  Value in Trimers of LHCII.** The second hyperpolarizability of LHCII complexes was obtained by measuring the THG intensity ratio of LHCII trimers at different concentrations. The hyperpolarizability is usually assigned to a single molecule. In our study we defined the effective second hyperpolarizability of a whole pigment–protein complex, which contains both chlorophyll and carotenoid pigments. The effective second hyperpolarizability of LHCII trimers was obtained with solubilized LHCII in 0.025% v/v Triton X-100. At this detergent concentration the LHCII was predominantly in the trimeric form when chlorophyll *a* + *b* concentration below 80  $\mu$ g/mL was used. At higher concentrations of the pigment–protein complex, LHCII was found to aggregate into larger structures. The aggregation state of LHCII was monitored using CD spectroscopy.<sup>20</sup> The THG signal for the LHCII suspension–glass interface and the glass–air interface of a capillary tube was found for a number of concentrations up to 100  $\mu$ g/mL of chlorophylls *a* + *b* (Figure 3a).

The THG intensity ratio increases with chlorophyll concentration, reminiscent of a similar dependence for chlorophyll *a* and chlorophyll *b*. Previous THG intensity ratio data of chlorophylls in acetone solvent also showed an increase in the THG intensity ratio with increasing concentration.<sup>17</sup> The refractive indices of the trimeric LHCII suspensions were found at 1028 and 343 nm (Figure 3b). LHCII does not absorb at 1028 nm; however, it absorbs at 343 nm. The third harmonic wavelength is near LHCII absorption resonance and as a result, the refractive index of suspensions containing trimeric LHCII decreases with increasing concentration.

The  $\chi^{(3)}$  plot of trimeric LHCII decreases with increasing chlorophyll *a* + *b* concentration (Figure 3c). This suggests that the THG emitted from LHCII has the opposite phase with respect to the THG emitted from the buffer solution. This corresponds well with previous data that showed that the  $\chi^{(3)}$  plots of chlorophylls *a* and *b* in acetone decrease with increasing concentration while the  $\chi^{(3)}$  plots of xanthophylls in acetone increase with increasing concentration.<sup>17</sup> As a result, chlorophylls *a* and *b* have negative  $\gamma$  values while xanthophylls have positive  $\gamma$  values.

From the  $\chi^{(3)}$  plot of trimeric LHCII, the  $\gamma$  value was extracted and found to be  $(-1600 \pm 400) \times 10^{-41} \text{ m}^2 \text{V}^{-2}$ . This value was compared to an estimated  $\gamma$  value for the LHCII trimer, which consisted of the summation of individual xanthophylls and chlorophyll molecules. X-ray crystallographic

studies of LHCII have concluded that a monomer of LHCII contains eight chlorophyll *a*, six chlorophyll *b*, and four xanthophyll molecules (two lutein, one neoxanthin, and one violaxanthin).<sup>30,31</sup> Therefore, the estimated  $\gamma$  value for LHCII was obtained by the addition of individual  $\gamma$  values of pigments corresponding to an LHCII trimer. The estimated  $\gamma$  value for trimeric LHCII was found to be  $(-3800 \pm 100) \times 10^{-41} \text{ m}^2 \text{V}^{-2}$ , which has an absolute value slightly larger than the experimentally measured  $\gamma$  value of LHCII (Table 1). In this

**Table 1.** The  $\gamma$  Value of LHCII Measured by the THG Ratio Technique, Individual  $\gamma$  Values of Carotenoids and Chlorophylls Found in LHCII, and the  $\gamma$  Value of LHCII Calculated from Individual  $\gamma$  Values of Carotenoids and Chlorophylls

harmonophore	$\gamma$ ( $10^{-41} \text{ m}^2 \text{V}^{-2}$ )
measured LHCII trimer	$-1600 \pm 400$
estimated LHCII trimer	$-3800 \pm 500^a$
violaxanthin <sup>16</sup>	$+3.1 \pm 0.6$
neoxanthin <sup>16</sup>	$+8 \pm 2$
lutein <sup>16</sup>	$+1.4 \pm 0.3$
chlorophyll <i>a</i> <sup>17</sup>	$-100 \pm 20$
chlorophyll <i>b</i> <sup>17</sup>	$-80 \pm 10$

<sup>a</sup>The  $\gamma$  value of the LHCII trimer was estimated by the addition of individual  $\gamma$  values for 24 chlorophyll *a*, 18 chlorophyll *b*, 6 lutein, 3 neoxanthin, and 3 violaxanthin molecules dissolved in acetone.<sup>16,17</sup>

estimation, the presence of polypeptide chains and lipids in the LHCII protein was ignored because the  $\gamma$  values of amino acids<sup>32</sup> and lipids are small, and therefore their  $\gamma$  values were not expected to contribute significantly to the overall  $\gamma$  value of LHCII.

A difference between the experimentally measured and estimated  $\gamma$  values of the LHCII trimer is expected based on the variation in molecular environment and interaction between specifically oriented pigments in the pigment–protein complexes versus randomly oriented pigments in organic solvents. The  $\gamma$  values of xanthophylls and chlorophylls are measured in an acetone environment, while inside LHCII, the pigments experience a different dielectric environment of the protein. This change in environment leads to two effects, a slight change in the ground state wave function of the molecules, which influences the nonlinear optical properties, as well as a shift in the index of refraction at the fundamental and third harmonic

wavelength. The change in the environment has been exemplified by the alteration of the extinction coefficients, as has been shown to vary for chlorophyll *b* and xanthophylls in the LHCII protein and when present in acetone.<sup>33</sup> The excitonic interaction between chlorophyll and xanthophyll molecules is also expected to yield a deviation from the additive  $\gamma$  value. In fact the nonlinear optical properties of pigment molecules are characterized by the second hyperpolarizability tensor, and therefore molecular interactions are very sensitive to the orientation of pigments in pigment–protein complexes. On the other hand, the LHCII second hyperpolarizability averages to an effective scalar value in the suspension. Therefore, the THG ratio technique measures the effective  $\gamma$  value of LHCII. By contrast,  $\gamma$  measurements of chlorophylls and xanthophylls in solution results in an overall orientationally averaged  $\gamma$  values for each pigment.

Second hyperpolarizability values can also be sensitive to solvent polarity where, for instance, it has been shown that the  $\gamma$  values of carotenoids with donor–acceptor functional groups are largely affected by changes in solvent environment.<sup>34</sup> However, the  $\gamma$  values for other carotenoids tends to be similar in various solvents, and therefore changes in solvent polarity are not expected to largely affect the  $\gamma$  values of the xanthophylls studied. Conversely, the solvent effects on the  $\gamma$  values of chlorophylls are not fully known. One study explored the changes in  $\chi^{(3)}$  for the sulfonated zinc(II) 2,3-naphthalocyanine porphyrin (ZnNcS) in dimethyl sulfoxide (DMSO), dimethylformamide (DMF), and water.<sup>35</sup> Results showed that the  $\chi^{(3)}$  for ZnNcS in DMSO was much higher than  $\chi^{(3)}$  for ZnNcS in DMF and water, however,  $\gamma$  values could not be obtained as ZnNcS aggregates in DMF and water.<sup>35</sup> The authors concluded that solvent polarity and aggregation influences  $\chi^{(3)}$ .<sup>35</sup> Therefore,  $\chi^{(3)}$  measurements of chlorophylls are sensitive to its environment and may contribute to overall differences observed between measured and calculated  $\gamma$  values for LHCII.

Overall, the  $\chi^{(3)}$  measurements were achieved at a single wavelength. Therefore, if the absorption spectrum of LHCII shifts, the change in  $\chi^{(3)}$  will be detected, but it is uncertain whether an overall change in the amplitude of  $\chi^{(3)}$  occurs with various wavelengths. Future measurements should concentrate on studying  $\chi^{(3)}$  of LHCII at various wavelengths in order to understand the changes in  $\chi^{(3)}$  values due to the harmonophores environment in pigment–protein complexes and due to the interactions between the pigments.

**THG Ratio at Different Stoichiometries of Chlorophylls and Carotenoids.** In order to explore the effect of a mixture of negative and positive  $\gamma$  values of pigments in the LHCII trimer, different ratios of representative harmonophores for LHCII (chlorophyll *a* and  $\beta$ -carotene) were mixed in acetone solution (Figure 4). Although  $\beta$ -carotene is not present in LHCII,  $\beta$ -carotene was chosen, as its  $\gamma$  value  $((4.9 \pm 0.8) \times 10^{-41} \text{ m}^2 \text{ V}^{-2})^{16,17}$  is representative of the average  $\gamma$  value of the xanthophylls present in LHCII (Table 1). These experiments served as a control by which one can test the accuracy of the THG ratio technique, and observe that in a solution, the second hyperpolarizabilities of chlorophyll and  $\beta$ -carotene are additive.

In Figure 4, the THG ratio of pure chlorophyll *a* in acetone increases with increasing concentration similar to LHCII in Figure 3a. At a ratio of 1:0.27 (15:4) chlorophyll *a* (Chl *a*) to  $\beta$ -carotene ( $\beta$ -car), which is representative of the ratio between chlorophylls and xanthophylls in LHCII, the THG ratio also increases and shows no significant difference to pure chlorophyll *a*. Therefore, this demonstrates that the effective

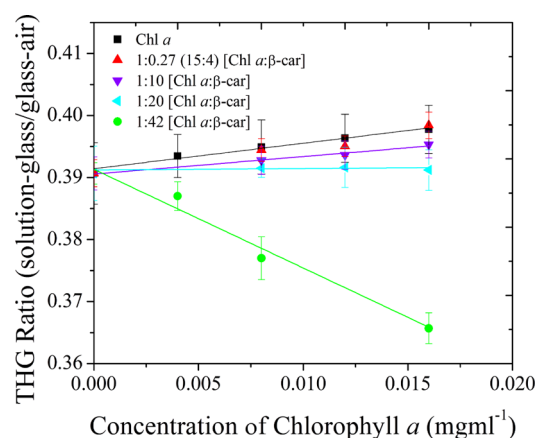


**Figure 4.** The THG intensity ratio for a solution of chlorophyll *a* (Chl *a*) in acetone, and a mixture of  $\beta$ -carotene ( $\beta$ -car) and Chl *a* in acetone as plotted against Chl *a* concentration. The ratio of Chl *a* to  $\beta$ -car was kept the same in each experimental curve. The ratio 1:0.27 (15:4) Chl *a* to  $\beta$ -car in solution is representative of the number of carotenoids to chlorophylls in LHCII. At a ratio of 1:10 Chl *a* to  $\beta$ -car, the THG ratio increases while at a ratio of 1:20, the THG ratio remains constant and at a ratio of 1:42, the THG ratio decreases.

$\gamma$  value of LHCII should predominantly originate from chlorophylls and the influence of carotenoids should be minimal. When the mixture contains a ratio of 1:10 chlorophyll *a* to  $\beta$ -carotene, the THG ratio also increases with increasing chlorophyll *a* concentration however; the slope of this line is more gradual than the slope of pure chlorophyll *a*. Therefore, at this ratio, the effective  $\gamma$  value of the mixture is smaller than the  $\gamma$  value of pure chlorophyll *a*. At a ratio of 1:20 chlorophyll *a* to  $\beta$ -carotene, the THG ratio remains constant. Since the  $\gamma$  values are the same in magnitude, but opposite in sign, THG generated from chlorophyll *a* cancels with the THG generated from  $\beta$ -carotene molecules, and the overall THG intensity ratio remains the same as the solvent. This experiment confirms that at 1028 nm fundamental wavelength, the magnitude of the  $\gamma$  value for 1 chlorophyll *a* molecule corresponds to the magnitude of the  $\gamma$  value for 20  $\beta$ -carotene molecules. At high concentrations of  $\beta$ -carotene such as at a ratio of 1:42 chlorophyll *a* to  $\beta$ -carotene, the THG ratio decreases with increasing chlorophyll *a* concentration as seen in Figure 4. This trend is reminiscent of the THG ratio of pure  $\beta$ -carotene.<sup>17</sup>

Overall, THG ratio studies of a mixture of carotenoids and chlorophylls further demonstrate that the  $\gamma$  value of carotenoids and chlorophylls are opposite in sign, and the  $\gamma$  value of chlorophylls are much larger than carotenoids. Therefore, it is predicted that larger  $\gamma$  values should be observed in pigment–protein complexes that contain only chlorophyll pigments.

## CONCLUSIONS

The  $\gamma$  value of the trimeric light-harvesting chlorophyll *a/b* pigment–protein complex of photosystem II isolated from pea (*Pisum sativum*) plants was investigated by the THG ratio technique and found to be  $(-1600 \pm 400) \times 10^{-41} \text{ m}^2 \text{ V}^{-2}$ . The  $\gamma$  value of LHCII at the fundamental wavelength 1028 nm is negative and predominantly originates from the chlorophylls. The experimental  $\gamma$  value of LHCII trimers was found to be smaller than the estimated  $\gamma$  value from the corresponding stoichiometry summation of individual  $\gamma$  values of chlorophylls and xanthophylls in acetone. This difference is attributed to the differing molecular orientations of pigments in LHCII versus an

isotropic solution as well as inter-pigment interactions that exist within LHCII. It is also shown that aggregation of LHCII leads to an increase in the  $\chi^{(3)}$  values, the same effect observed for hematoxylin aggregates.<sup>28</sup>

## ■ ASSOCIATED CONTENT

### ■ Supporting Information

Plot consisting of the multiphoton excitation fluorescence intensities of LHCII as well as xanthophylls and chlorophyll *a* in acetone at different excitation laser intensities. This material is available free of charge via the Internet at <http://pubs.acs.org>.

## ■ AUTHOR INFORMATION

### Corresponding Author

\*Mail: Department of Chemical and Physical Sciences, University of Toronto Mississauga, 3359 Mississauga Rd. N., Mississauga, ON, Canada L5L 1C6. Tel.: +1 905 828 3821. Fax: +1 905 828-5425. E-mail: [virgis.barzda@utoronto.ca](mailto:virgis.barzda@utoronto.ca).

### Notes

The authors declare no competing financial interest.

## ■ ACKNOWLEDGMENTS

The authors gratefully acknowledge Professor Jumi A. Shin, University of Toronto, for access to a CD spectrometer, Professor Ingo Ensminger and Laura Junker, University of Toronto, for donating chlorophyll *a*, and Marianne Kalich, University of Toronto, for assistance in growing pea (*Pisum sativum*) plants. The research was supported by the Natural Science and Engineering Research Council of Canada (NSERC). D.T. also kindly acknowledges support from NSERC.

## ■ ABBREVIATIONS

MPF, multiphoton excitation fluorescence; SHG, second harmonic generation; THG, third harmonic generation

## ■ REFERENCES

- (1) Hermann, J. P.; Ducuing, J. Third-Order Polarizabilities of Long-Chain Molecules. *J. Appl. Phys.* **1974**, *45*, 5100–5102.
- (2) Marder, S. R.; Torruellas, W. E.; Blanchard-Desce, M.; Ricci, V.; Stegeman, G. I.; Gilmour, S.; Brédas, J. L.; Li, J.; Bublitz, G. U.; Boxer, S. G. Large Molecular Third-Order Optical Nonlinearities in Polarized Carotenoids. *Science* **1997**, *276*, 1233–1236.
- (3) Senge, M. O.; Fazekas, M.; Notaras, E. G. A.; Blau, W. J.; Zawadzka, M.; Locos, O. B.; Mhuirheartaigh, E. M. N. Nonlinear Optical Properties of Porphyrins. *Adv. Mater.* **2007**, *19*, 2737–2774.
- (4) Muller, M.; Squier, J.; Wilson, K. R.; Brakenhoff, G. J. 3D Microscopy of Transparent Objects Using Third-Harmonic Generation. *J. Microsc. (Oxford, U. K.)* **1998**, *191*, 266–274.
- (5) Squier, J. A.; Muller, M.; Brakenhoff, G. J.; Wilson, K. R. Third Harmonic Generation Microscopy. *Opt. Express* **1998**, *3*, 315–324.
- (6) Millard, A. C.; Wiseman, P. W.; Fittinghoff, D. N.; Wilson, K. R.; Squier, J. A.; Muller, M. Third-Harmonic Generation Microscopy by Use of a Compact, Femtosecond Fiber Laser Source. *Appl. Opt.* **1999**, *38*, 7393–7397.
- (7) Chu, S. W.; Chen, I. H.; Liu, T. M.; Chen, P. C.; Sun, C. K.; Lin, B. L. Multimodal Nonlinear Spectral Microscopy Based on a Femtosecond Cr:Forsterite Laser. *Opt. Lett.* **2001**, *26*, 1909–1911.
- (8) Cisek, R.; Spencer, L.; Prent, N.; Zigmantas, D.; Espie, G.; Barzda, V. Optical Microscopy in Photosynthesis. *Photosynth. Res.* **2009**, *102*, 111–141.
- (9) Barzda, V. Non-linear Contrast Mechanisms for Optical Microscopy. In *Biophysical Techniques in Photosynthesis*; Aartsma, T. J., Matysik, J., Eds.; Springer: Dordrecht, Netherlands, 2008; Vol. 2; pp 35–54.
- (10) Prent, N.; Cisek, R.; Greenhalgh, C.; Sparrow, R.; Rohitlall, N.; Milkereit, M.; Green, C.; Barzda, V. Applications of Nonlinear Microscopy for Studying the Structure and Dynamics in Biological Systems. *Proc. SPIE—Int. Soc. Opt. Eng.* **2005**, *5971*, 5971061.
- (11) Thornber, J. P. Chlorophyll-Proteins: Light-Harvesting and Reaction Center Components of Plants. *Annu. Rev. Plant Phys.* **1975**, *26*, 127–158.
- (12) van Grondelle, R.; Monshouwer, R.; Valkunas, L. Photo-synthetic Light-Harvesting. *Ber. Bunsen Phys. Chem.* **1996**, *100*, 1950–1957.
- (13) van Grondelle, R.; Novoderezhkin, V. I. Energy Transfer in Photosynthesis: Experimental Insights and Quantitative Models. *Phys. Chem. Chem. Phys.* **2006**, *8*, 793–807.
- (14) Scholes, G. D.; Fleming, G. R.; Olaya-Castro, A.; van Grondelle, R. Lessons from Nature about Solar Light Harvesting. *Nat. Chem.* **2011**, *3*, 763–774.
- (15) van Amerongen, H.; van Grondelle, R. Understanding the Energy Transfer Function of LHCII, the Major Light-Harvesting Complex of Green Plants. *J. Phys. Chem. B* **2001**, *105*, 604–617.
- (16) Tokarz, D.; Cisek, R.; Garbaczewska, M.; Sandkuijl, D.; Qiu, X.; Stewart, B.; Levine, J. D.; Fekl, U.; Barzda, V. Carotenoid Based Bio-compatible Labels for Third Harmonic Generation Microscopy. *Phys. Chem. Chem. Phys.* **2012**, *14*, 10653–61.
- (17) Tokarz, D.; Cisek, R.; Prent, N.; Fekl, U.; Barzda, V. Measuring the Molecular Second Hyperpolarizability in Absorptive Solutions by the Third Harmonic Generation Ratio Technique. *Anal. Chim. Acta* **2012**, *755*, 86–92.
- (18) Simidjiev, I.; Barzda, V.; Mustardy, L.; Garab, G. Isolation of Lamellar Aggregates of the Light-Harvesting Chlorophyll *a/b* Protein Complex of Photosystem II with Long-Range Chiral Order and Structural Flexibility. *Anal. Biochem.* **1997**, *250*, 169–175.
- (19) Arnon, D. I. Copper Enzymes in Isolated Chloroplasts - Polyphenoloxidase in Beta-Vulgaris. *Plant Physiol.* **1949**, *24*, 1–15.
- (20) Barzda, V.; Mustardy, L.; Garab, G. Size Dependency of Circular-Dichroism in Macroaggregates of Photosynthetic Pigment-Protein Complexes. *Biochemistry* **1994**, *33*, 10837–10841.
- (21) Greenhalgh, C.; Prent, N.; Green, C.; Cisek, R.; Major, A.; Stewart, B.; Barzda, V. Influence of Semicrystalline Order on the Second-Harmonic Generation Efficiency in the Anisotropic Bands of Myocytes. *Appl. Opt.* **2007**, *46*, 1852–1859.
- (22) Major, A.; Cisek, R.; Sandkuijl, D.; Barzda, V. Femtosecond Yb:KGd(WO<sub>4</sub>)<sub>2</sub> Laser with >100 nJ of Pulse Energy. *Laser Phys. Lett.* **2009**, *6*, 272–274.
- (23) Pillai, R. S.; Brakenhoff, G. J.; Muller, M. Analysis of the Influence of Spherical Aberration from Focusing Through a Dielectric Slab in Quantitative Nonlinear Optical Susceptibility Measurements Using Third-Harmonic Generation. *Opt. Express* **2006**, *14*, 260–269.
- (24) Shcheslavskiy, V.; Petrov, G.; Yakovlev, V. V. Nonlinear Optical Susceptibility Measurements of Solutions Using Third-Harmonic Generation on the Interface. *Appl. Phys. Lett.* **2003**, *82*, 3982–3984.
- (25) Kajzar, F.; Ledoux, I.; Zyss, J. Electric-Field-Induced Optical 2nd-Harmonic Generation in Polydiacetylene Solutions. *Phys. Rev. A* **1987**, *36*, 2210–2219.
- (26) Tykewinski, R. R.; Gubler, U.; Martin, R. E.; Diederich, F.; Bosshard, C.; Gunter, P. Structure-Property Relationships in Third Order Nonlinear Optical Chromophores. *J. Phys. Chem. B* **1998**, *102*, 4451–4465.
- (27) Cisek, R.; Prent, N.; Greenhalgh, C.; Sandkuijl, D.; Tuer, A.; Major, A.; Barzda, V. Multicontrast Nonlinear Imaging Microscopy. In *Biochemical Applications of Nonlinear Optical Spectroscopy*; Yakovlev, V. V., Ed.; CRC Press: New York, 2009; pp 71–102.
- (28) Tuer, A.; Tokarz, D.; Prent, N.; Cisek, R.; Alami, J.; Dumont, D. J.; Bakueva, L.; Rowlands, J.; Barzda, V. Nonlinear Multicontrast Microscopy of Hematoxylin-and-Eosin-Stained Histological Sections. *J. Biomed. Opt.* **2010**, *15*, 026018.
- (29) Hobe, S.; Prytulla, S.; Kuhlbrandt, W.; Paulsen, H. Trimerization and Crystallization of Reconstituted Light-Harvesting Chlorophyll *a/b* Complex. *EMBO J.* **1994**, *13*, 3423–3429.

- (30) Liu, Z. F.; Yan, H. C.; Wang, K. B.; Kuang, T. Y.; Zhang, J. P.; Gui, L. L.; An, X. M.; Chang, W. R. Crystal Structure of Spinach Major Light-Harvesting Complex at 2.72 Å Resolution. *Nature* **2004**, *428*, 287–292.
- (31) Standfuss, R.; van Scheltinga, A. C. T.; Lamborghini, M.; Kuhlbrandt, W. Mechanisms of Photoprotection and Nonphotochemical Quenching in Pea Light-Harvesting Complex at 2.5 Å Resolution. *EMBO J.* **2005**, *24*, 919–928.
- (32) Tokarz, D.; Tuer, A.; Cisek, R.; Krouglov, S.; Barzda, V. J. *Phys. Chem. Solids* **2010**, *256*, 012015.
- (33) Croce, R.; Cinque, G.; Holzwarth, A. R.; Bassi, R. The Soret Absorption Properties of Carotenoids and Chlorophylls in Antenna Complexes of Higher Plants. *Photosynth. Res.* **2000**, *64*, 221–231.
- (34) Marder, S. R.; Perry, J. W.; Bourhill, G.; Gorman, C. B.; Tiemann, B. G.; Mansour, K. Relation Between Bond-Length Alternation and 2nd Electronic Hyperpolarizability of Conjugated Organic-Molecules. *Science* **1993**, *261*, 186–189.
- (35) Fu, G.; Yoda, T.; Kasatani, K. Third-Order Optical Non-linearities of Several Naphthalocyanines and Porphyrins Measured by the Resonant Femtosecond DFWM Technique. *Proc. SPIE–Int. Soc. Opt. Eng.* **2005**, *5646*, 471–479.